Evaluating the Effectiveness of Compliant Leading Edge Control Surfaces on an Oblique Flying Wing for Directional Control

Joshua Deslich *, Peter Flick †, and Chris M. Meckstroth ‡
University of Dayton Research Institute, Dayton, OH, USA, 45469

Doug Szczublewski §
Wright-Patterson Air Force Base, Dayton, OH, USA, 45433

The Oblique Flying Wing configuration (OFW) has historically been a difficult configuration to control. Lacking empennage control surfaces, control authority is limited and has led to many compromises in aerodynamic efficiency. Taking lessons learned from legacy flight test programs such as the X-53 Active Aeroelastic Wing (AAW) program, the benefits of including leading edge control surfaces for maneuvers is evident. With maturing compliant structures technology, integration of a compliant leading edge into the early stage design process of an OFW can aid in improving the controllability and aerodynamic performance. Utilizing parametric geometry tools, gradient based optimization, and RANS CFD, the over-determined rigid trim problem can be solved. Two OFW configurations, with and without leading edge compliant control surfaces, are compared at three flight conditions. Evaluating the ability of each configuration to satisfy the trim constraints and produce the required yaw moments will determine the effectiveness of including compliant leading edge control surfaces on an OFW.

I. Nomenclature

C_L	=	Lift Coefficient
C_D	=	Drag Coefficient
C_S	=	Side Force Coefficient
C_l	=	Rolling Moment Coefficient
C_m	=	Pitching Moment Coefficient
C_n	=	Yawing Moment Coefficient
c	=	Chord (m)
$\overline{c}$	=	Mean Aerodynamic Chord (m)
b	=	Span (m)
Λ	=	Slew Angle (°)
α	=	Angle of attack (°)
δ_i	=	Control Surface Deflection (°)

II. Introduction

The Oblique Flying Wing (OFW) is a unique configuration that lends itself to many aerodynamic advantages made possible through asymmetric sweep and asymmetries in the planform. Asymmetric sweep, or slew, allows for the OFW to reduce its span and frontal area, reducing the wave drag at transonic and supersonic flight conditions [1, 2]. Over the course of a mission, an OFW can achieve various slew angles depending on the flight regime. In low subsonic flight regimes, a low slew angle will provide efficient lift production, but in supersonic flight an increased slew angle also

*Associate Research Engineer, joshua.deslich.ctr@us.af.mil, University of Dayton Research Institute, AIAA Member
†Distinguished Research Engineer, peter.flick.1.ctr@us.af.mil, University of Dayton Research Institute
‡Research Engineer, Christopher.Meckstroth@udri.udayton.edu, University of Dayton Research Institute, AIAA Member
§Aerospace Engineer, douglas.szczublewski@us.af.mil, AFRL/RQVC

for reduced wave drag. This makes an OFW a very versatile configuration capable of efficient flight for a variety of missions.

In addition to varying slew angle, an OFW by definition does not have tail empennages, again reducing the drag on the configuration. While efficiency is increased, the absence of empennage surfaces makes an OFW difficult to control directionally and brings about extra design considerations for longitudinal control. There are only a few configurations that have attempted an oblique wing, with the most notable example being the NASA AD-1. Even with the use of conventional tail empennage control surfaces, the AD-1 still experienced many control deficiencies [3]. During flight testing, it was found that there was a strong cross-coupling of pitch and roll which was exacerbated at high slew angles, degrading the handling qualities. In addition to the cross-coupling, roll maneuvers were difficult at high slew angles due to deficiencies in directional control authority. If the vehicle was not properly trimmed with the rudder, roll control authority was diminished, preventing the completion of the maneuver. In all cases, test pilots noted that the AD-1 experienced degraded handling at high slew angles and that for trimmed flight, the AD-1 experienced lateral instabilities. Overall, the AD-1 program brought to light many of the challenges when developing an oblique wing and even with conventional control systems, achieving acceptable handling at high slew angles was difficult.

Since the AD-1, other configurations were developed that do not have conventional empennage control surfaces, notably, the B-2 bomber. The B-2 utilizes split ailerons, or split rudders to gain directional control. This method of control primarily relies on drag production caused by the split ailerons separating the flow over the wing. In the case of an OFW, split ailerons have diminished control authority with increasing slew angle, limiting their effectiveness [4]. For a variable configuration such as an OFW, using a split aileron control device only provides control over a small flight envelope, which is why a different approach is needed when developing a control system for an OFW.

Active Aeroelastic Wing (AAW) research has shown that including spanwise leading edge control surfaces can reduce control deflections needed for trimmed flight. This is primarily driven by the stiffness reductions in the AAW, but even the baseline stiff wings show reduced control deflections for trim when the leading edge is considered [5]. Other objectives are achievable other than efficient trim such as increased control performance and reduced wing-root bending moment which was seen in the X-53 flight test program [6, 7].

A preceding effort to the AAW research was the Mission Adaptive Wing (MAW) program, which used the leading and trailing edge control surfaces to vary the camber of airfoil sections along the span. Like the AAW program, MAW showed that increased maneuverability was achievable with variable camber [8]. Using ideas from both MAW and AAW, the use of conformal control surfaces rather than conventional control surfaces can further reduce the control surface deflections required for trim and still gain the increased maneuverability [9]. Recent flight tests from NASA, AFRL, and Flexsys have shown the conformal, complaint control surfaces have real potential to improve air vehicle designs. The ability to tailor the spanwise wing loading to reduce wing-root bending moment can allow for lighter structures and improve overall mission performance [10].

In addition to reducing wing-root bending moment and other structural objectives, the complaint control surfaces on an OFW can be used to increase directional control. Developing an efficient method to alleviate the historical directional instabilities is a critical component in making an OFW a viable configuration. Recent work considering a rigid OFW has shown that many severe aerodynamic moments can be mitigated with a tailored geometric twist distribution [11]. Exchanging a fixed geometric twist distribution with compliant control surfaces allows for a variable geometry that could provide more control over a larger flight envelope.

With the benefits of compliant control surfaces on both leading and trailing edges, including them in the early design process can likely improve on the what was shown in the MAW and AAW efforts. The ultimate goal is to integrate aeroelastic effects with the trim analysis but for this paper, the scope of work is limited to understanding trim and control objectives on a rigid configuration. Using an OFW configuration based on artistic representations of the DARPA/Northop-Grumman Switchblade OFW planform, a baseline configuration without compliant leading edge control surfaces is compared to a configuration which utilizes the leading edge. There are many flight conditions that could benefit from a compliant leading edge such as drag reduction in level-flight, or minimization of wing-root bending moment for a pull-up maneuver. For this study, a series of 1-g flight conditions will be investigated with RANS CFD to evaluate the effectiveness of the leading edge to improve directional control. It is expected that the leading edge will have a significant impact on the directional control as recent work from NASA has shown the power of using different lift distributions to produce proverse directional control [12].

III. Methodology

A. Model Definition

The OFW configuration used in this study is based on artistic representations of the DARPA/Northrop-Grumman Switchblade planform [11]. Two configurations are evaluated, a baseline OFW with only trailing edge control surfaces, and a compliant configuration utilizing two compliant leading edge control surfaces. Both models are parametrically defined in Engineering Sketch Pad (ESP) to allow for rapid model generation and integration into the analysis environment [13]. Figure 1 shows the control surface conventions that are used along with the control variables to determine control surfaces deflection.

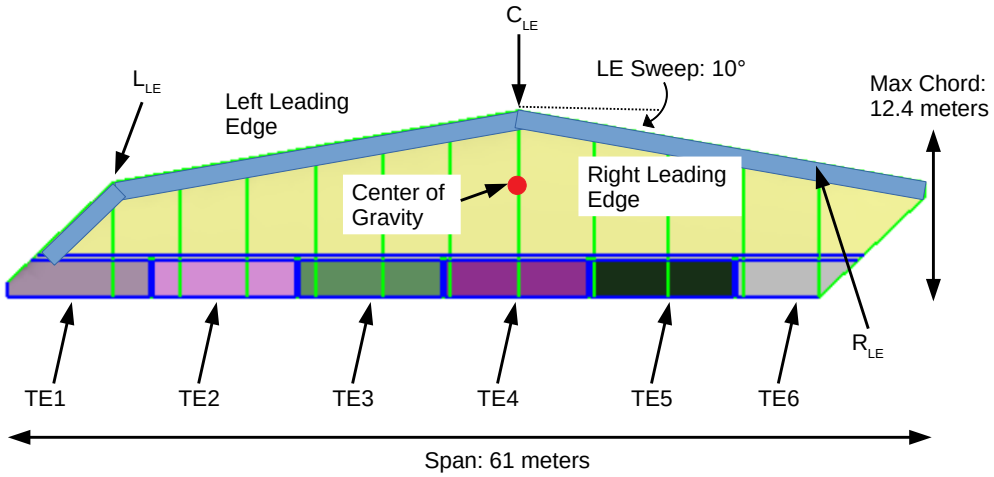

Fig. 1 OFW Model with Control Surfaces and Control Variables

The trailing edge control surfaces for both configurations are conventional with a single design parameter controlling the deflection angle of the surface. An example of a trailing control surface deflection is shown in Figure 2a. For the compliant leading edge control surfaces on the compliant configuration, three control points are defined as representative actuator locations. These actuator control points determine the local deflection of the leading edge control surface, and like the Flexsys ATE control surface, the leading edge control surface is linearly connected between the two control points. Beyond the outer most control points, L_{LE} and R_{LE}, the leading edge surface is linearly connected to the wingtip airfoil sections to provide a smooth transition between the control point and wingtip airfoils.

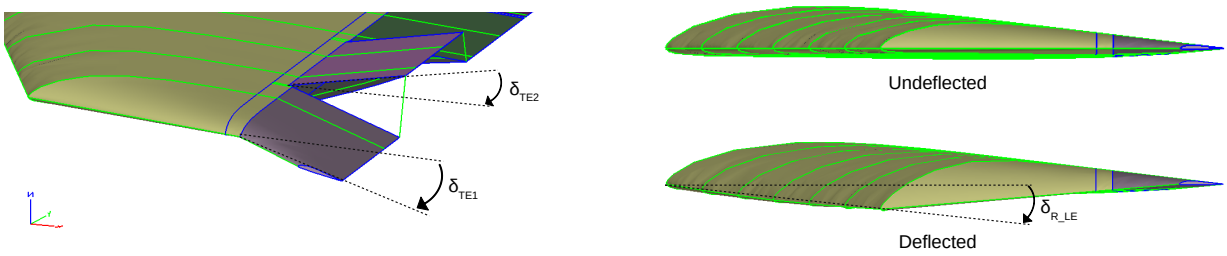

(a) Conventional Trailing Edge Control Surfaces **(b) Compliant Leading Edge Control Surfaces**

Fig. 2 Examples of Control Surface Deflections for an Oblique Flying Wing

The trailing edge control surfaces have a constant chord length of 20% of the maximum wing chord and the inboard

surfaces have equal spans. The two outboard trailing edge control surfaces TE1 and TE6 have slightly varied spans in comparison due to significant tapering at the wingtips. From analysis, the moment coefficients will be evaluated at the center of gravity (CG) location shown in Figure 1. At each flight condition, both OFW configurations will have a weight of 20,000 lbs and the CG location will remain at a constant location on the planform independent of slew angle.

B. Optimization Problem Definition

The optimization problem is developed to evaluate the benefits provided by a compliant leading edge on directional control in a 1-g flight condition. Historically, the aerodynamic performance was compromised over the entire flight regime to account for directional instabilities. Traditionally, trim analysis and trim optimization considers the lift/weight equilibrium and pitching moment equilibrium as the primary constraints. For most configurations this would be sufficient, but for an asymmetric OFW configuration, inclusion of the lateral (roll) moment coefficient as an equilibrium constraint is required. In addition to the rolling moment, the side force is required as an equilibrium constraint as it was identified in the AD-1 program that asymmetric sweep led to a strong side force. The optimization problem is shown in Equations (1) and (2) where α is the angle of attack and δ_i is the deflection angles of each control surface or control point. For the baseline OFW configuration, only the trailing edge control surfaces and angle of attack are considered for the optimization problem. The compliant configuration includes the three leading edge control points along with the trailing edge control surfaces and angle of attack. The objective of each optimization problem will be to maximize the yawing moment in a prescribed direction with a drag penalization to dissuade the use of drag to gain directional control. For a yaw left direction, the following problem is used to maximize the yaw left moment with a drag penalty.

$$\begin{aligned} \underset{\alpha,\delta_i}{\text{minimize}} \quad & C_n(\alpha,\delta_i) + C_D(\alpha,\delta_i) \\ \text{subject to} \quad & 0^\circ \le \alpha \le 10^\circ \\ & -10^\circ \le \delta_i \le 10^\circ \\ & -\sigma \le \sum F_i \le \sigma \\ & -\sigma \le \sum M_j \le \sigma \end{aligned} \tag{1}$$

Similarly, a yaw right direction is maximized with a drag penalty.

$$\begin{aligned} \underset{\alpha,\delta_i}{\text{minimize}} \quad & -C_n(\alpha,\delta_i) + C_D(\alpha,\delta_i) \\ \text{subject to} \quad & 0^\circ \le \alpha \le 10^\circ \\ & -10^\circ \le \delta_i \le 10^\circ \\ & -\sigma \le \sum F_i \le \sigma \\ & -\sigma \le \sum M_j \le \sigma \end{aligned} \tag{2}$$

It is expected that the optimizer will find a solution that can utilize some of the aerodynamic principles of proverse yaw, allowing for more efficient production of directional control. A numerical tolerance, σ, is placed on the force and moment equilibrium constraints to allow the optimizer to balance all the equilibrium constraints. The SLSQP gradient based optimization routine is used to determine a feasible solution for each problem subject to the tolerance on the constraints. Gradients are approximated using a forward finite-difference approximation with a step size of $\delta_i = 0.5$.

Three different flight conditions, detailed in Table 1, are investigated over a range of Mach numbers for each optimization problem. Each condition will have a separate mesh developed based on the Reynolds number of each flight condition. The meshes generated with AFRL3/4 will chosen based on the criteria of a maximum y+ value of 1 and on mesh independence.

Table 1 Test Matrix for Trim Flight Conditions

Trim Points	Mach Number	Slew Angle - Degrees	Altitude - Feet	Reynolds Number
1	0.30	0.0	5000	60,087,442
2	0.75	45.0	25000	119,097,772
3	1.40	65.0	40000	201,143,900

C. Optimization and Computational Environment

The execution the proposed trim analysis problems utilizes a series of computational tools to enable rapid geometric modeling, meshing, and analysis. ESP is used to model the OFW configurations as it is integrated into a Computational Analysis Prototype Synthesis (CAPS) framework which utilizes geometric parameters and meta-data in the ESP models for analysis [13, 14]. The optimization problems will be driven using OpenMDAO where CAPS and pyCAPS are used to link the optimization design variables with the geometric parameters [15, 16]. This integrated OpenMDAO/pyCAPS/ESP framework creates an interconnected system which will maintain consistent definitions for design and analysis parameters as well as facilitate the approximation of gradients and objective function evaluation. An XDSM diagram is shown in Figure 3 to show the integration of the miriade of computational tools which are integrated with OpenMDAO and pyCAPS.

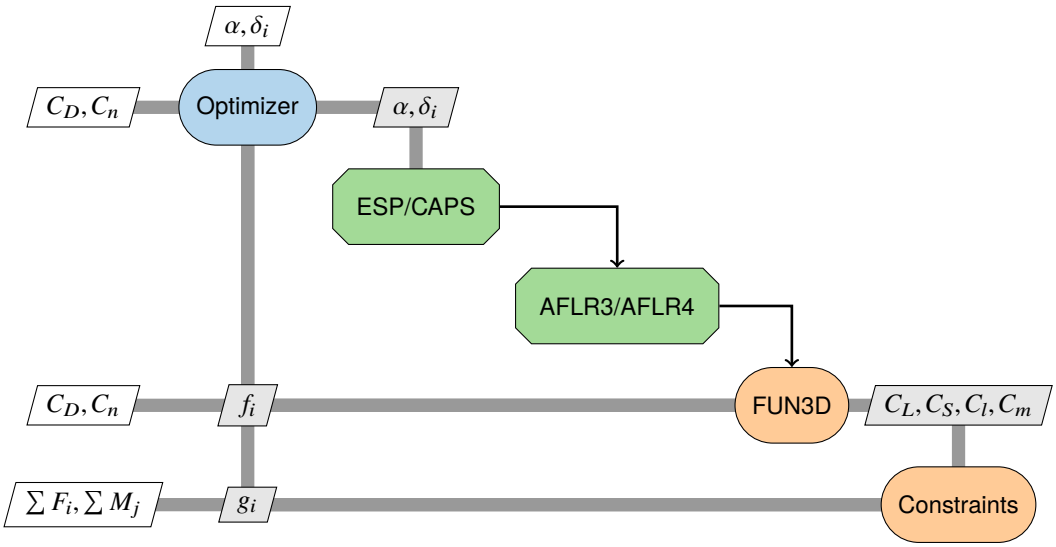

Fig. 3 XDSM for Trim Optmization Environment [17]

For meshing the geometry from ESP, automated meshing tools AFLR3 and AFLR4 are utilized within the CAPS environment to generated the required surface, boundary-layer, and volume meshes [18, 19]. FUN3D (Fully Unstructured Navier-Stokes) is used to solve for the integrated forces and moments about the approximated CG location and then pass the results onto OpenMDAO where the constraints and objective function can be evaluated [20].

D. FUN3D Solution Parameters

The CFD RANS problem was developed to account for the Mach and viscous effects that the OFW will experience at many of its flight conditions. Initially, the steady, compressible, and turbulent Navier-Stokes equations are used with the Spalart-Allmaras turbulence model [21]. A freestream turbulence value of 3.0 is used for the SA turbulence model, with a freestream turbulence intensity of -0.001, and uses the linear Reynolds stress model.

Flux limiters are used in the solution setup, utilizing the dissipative LDFSS method for the inviscid flux residual. The van Leer construction is used for the Jacobian and the *hvanleer* flux limiter is used. A scheduled CFL number is

initialized at 0.1 and then linearly increased to 20.0 over 1000 iterations.

E. Mesh Convergence Study

A mesh convergence study is performed to determine the automated meshing parameters required to produce physical and realistic solutions. In doing this, a computational domain is created to resolve the relevant flow physics in order to accurately determine the integrated forces and moments on the OFW. Initially, the mesh convergence study was performed using the aforementioned OFW configuration with no control surface deflections. Figure 4 shows that with increasing mesh density, the solution does not significantly change, but this is for the simplest configuration that is expected. A subsequent mesh convergence study will be performed to show mesh independence for an OFW configuration with deflected control surfaces. This will aid in developing a robust set of meshing parameters to be used throughout the optimization process.

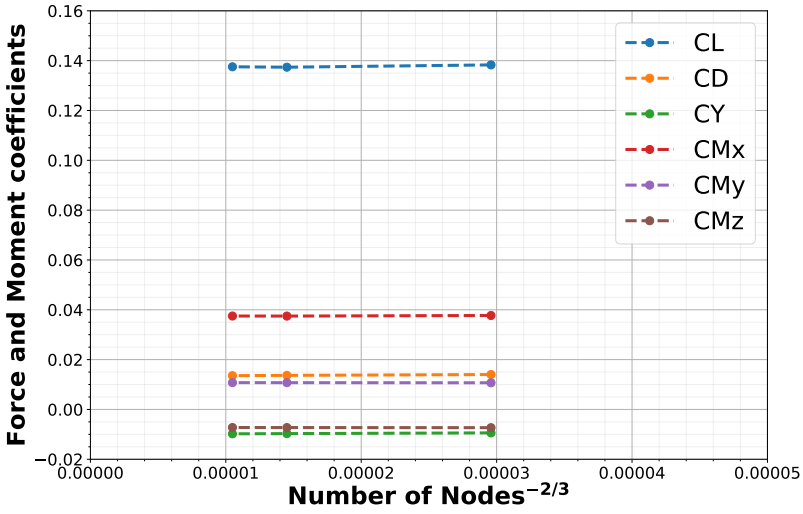

Fig. 4 Preliminary Grid Convergence Study using AFLR3 and AFLR4.

Aside from a mesh convergence study, a boundary-layer mesh was developed to provide a y+ spacing of less than one for the first node off the surface. Figures 5a and 5b show the y+ values for the fine mesh CFD solution.

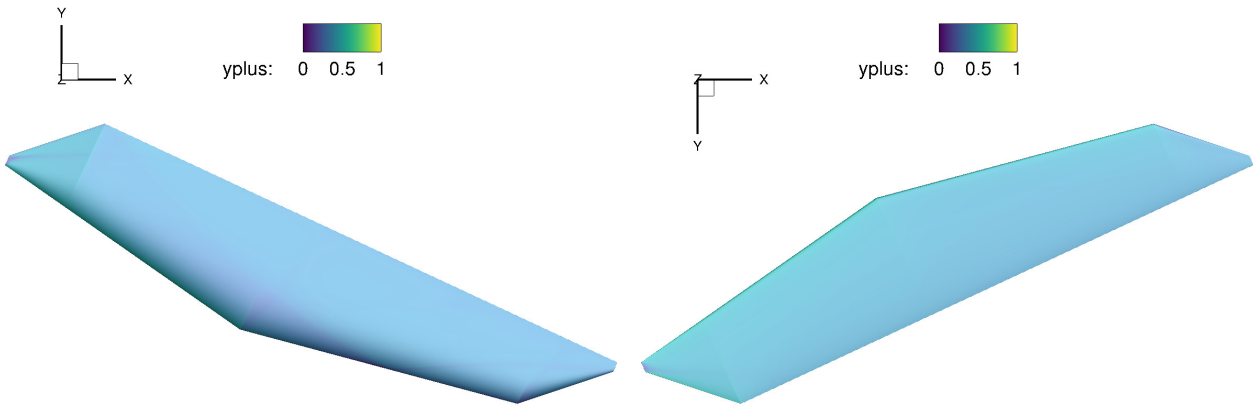

(a) Top OFW Planform **(b) Bottom OFW Planform**

Fig. 5 Planform Views of y+ Values for Fine Grid RANS Solution.

IV. Results

V. Conclusions

Note to Reviewer: Results and conclusions will be included in the final manuscript detailing the differences in performance between configurations at the conditions tested.

VI. Acknowledgments

This paper is cleared for Public Release, Distribution Unlimited. Case number: 88ABW-2020-1869

References

[1] Jones, R. T., "The oblique wing—aircraft design for transonic and low supersonic speeds," *Acta Astronautica*, Vol. 4, No. 1-2, 1977, pp. 99–109. https://doi.org/10.1016/0094-5765(77)90035-2.

[2] Jones, R. T., "Reduction of wave drag by antisymmetric arrangement of wings and bodies." *AIAA Journal*, Vol. 10, No. 2, 1972, pp. 171–176. https://doi.org/10.2514/3.6555.

[3] Sim, A. G., and Curry, R. E., "Flight characteristics of the AD-1 oblique-wing research aircraft," 1985. NASA TP-2223.

[4] Desktop-Aeronautics, "Oblique Flying Wings: An Introduction and White Paper," 2005.

[5] Andersen, G., Forster, E., Kolonay, R., and Eastep, F., "Multiple control surface utilization in active aeroelastic wing technology," *Journal of aircraft*, Vol. 34, No. 4, 1997, pp. 552–557. https://doi.org/10.2514/2.2208.

[6] Pendleton, E., Flick, P., Paul, D., Voracek, D., Reichenbach, E., and Griffin, K., "The X-53 a summary of the active aeroelastic wing flight research program," *48th AIAA/ASME/ASCE/AHS/ASC Structures, Structural Dynamics, and Materials Conference*, 2007, p. 1855. https://doi.org/10.2514/6.2007-1855.

[7] Zink, P. S., Mavris, D. N., and Raveh, D. E., "Maneuver trim optimization techniques for active aeroelastic wings," *Journal of Aircraft*, Vol. 38, No. 6, 2001, pp. 1139–1146. https://doi.org/10.2514/6.2000-1330.

[8] Bonnema, K., and Smith, S., "AFTI/F-111 mission adaptive wing flight research program," *4th Flight Test Conference*, 1988, p. 2118. https://doi.org/10.2514/6.1988-2118.

[9] Xie, J., Yang, Z., and Guo, S., "A flexible wing with conformal control surfaces for optimum trim of a tailless air vehicle," *51st AIAA/ASME/ASCE/AHS/ASC Structures, Structural Dynamics, and Materials Conference 18th AIAA/ASME/AHS Adaptive Structures Conference 12th*, 2010, p. 2713. https://doi.org/10.2514/6.2010-2713.

[10] Kota, S., Flick, P., and Collier, F. S., "Flight Testing of FlexFloilTM Adaptive Compliant Trailing Edge," *54th AIAA Aerospace Sciences Meeting*, 2016, p. 0036. https://doi.org/10.2514/6.2016-0036.

[11] Deslich, J., Gunasekaran, S., Flick, P., and Szczublewski, D., "Effects of spanloading and slew angle on an Oblique Flying Wing," *AIAA Scitech 2020 Forum*, 2020, p. 0532. https://doi.org/10.2514/6.2020-0532.

[12] Bowers, A. H., Murillo, O. J., Jensen, R. R., Eslinger, B., and Gelzer, C., "On wings of the minimum induced drag: Spanload implications for aircraft and birds," 2016. NASA TP-2016-219072.

[13] Haimes, R., and Dannenhoffer, J., "The engineering sketch pad: A solid-modeling, feature-based, web-enabled system for building parametric geometry," *21st AIAA Computational Fluid Dynamics Conference*, 2013, p. 3073. https://doi.org/10.2514/6.2013-3073.

[14] Alyanak, E., Durscher, R., Haimes, R., Dannenhoffer, J., Bhagat, N., and Allison, D., "Multi-fidelity Geometry-centric Multi-disciplinary Analysis for Design," *AIAA Modeling and Simulation Technologies Conference*, American Institute of Aeronautics and Astronautics, 2016. https://doi.org/10.2514/6.2016-4007.

[15] Durscher, R. J., and Reedy, D., "pyCAPS: A Python Interface to the Computational Aircraft Prototype Syntheses," *AIAA Scitech 2019 Forum*, 2019, p. 2226. https://doi.org/10.2514/6.2019-2226.

[16] Heath, C., and Gray, J., "OpenMDAO: framework for flexible multidisciplinary design, analysis and optimization methods," *53rd AIAA/ASME/ASCE/AHS/ASC Structures, Structural Dynamics and Materials Conference 20th AIAA/ASME/AHS Adaptive Structures Conference 14th AIAA*, 2012, p. 1673. https://doi.org/10.2514/6.2012-1673.

[17] Lambe, A. B., and Martins, J. R. R. A., "Extensions to the Design Structure Matrix for the Description of Multidisciplinary Design, Analysis, and Optimization Processes," *Structural and Multidisciplinary Optimization*, Vol. 46, 2012, pp. 273–284. doi:10.1007/s00158-012-0763-y.

[18] Marum, D. L., and Weatherill, N. P., "Unstructured Grid Generation Using Iterative Point Insertion and Local Reconnection," *AIAA Journal*, Vol. 33, No. 9, 1995, pp. 1619–1625. https://doi.org/10.2514/3.12701.

[19] Marum, D. L., "Unstructured Grid Generation Using Automatic Point Insertion and Local Reconnection," *Handbook of grid generation*, 1998, pp. 18–1. Edited by J.F Thompson, B. Soni, and N.P. Weatherill, CRC Press.

[20] Biedron, R. T., Carlson, J.-R., Derlaga, J. M., Gnoffo, P. A., Hammond, D. P., Jones, W. T., Kleb, B., Lee-Rausch, E. M., Nielsen, E. J., Park, M. A., et al., "FUN3D Manual: 13.4," 2018. NASA/TM–2018–220096.

[21] Spalart, P., and Allmaras, S., "A one-equation turbulence model for aerodynamic flows," *30th aerospace sciences meeting and exhibit*, 1992, p. 439. https://doi.org/10.2514/6.1992-439.